

SCIENTIFIC REPORTS

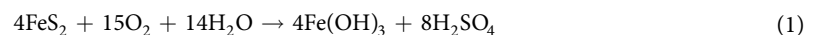
OPEN

Sulphuric acid-mediated weathering on Taiwan buffers geological atmospheric carbon sinks

T. M. Blattmann¹, S.-L. Wang^{2,3}, M. Lupker¹, L. Märki¹, N. Haghypour¹, L. Wacker⁴, L.-H. Chung⁵, S. M. Bernasconi¹, M. Plötze⁶ & T. I. Eglinton¹

The chemical composition of the Gaoping River in Taiwan reflects the weathering of both silicate and carbonate rocks found in its metasedimentary catchment. Major dissolved ion chemistry and radiocarbon signatures of dissolved inorganic carbon (DIC) reveal the importance of pyrite-derived sulphuric acid weathering on silicates and carbonates. Two-thirds of the dissolved load of the Gaoping River derives from sulphuric acid-mediated weathering of rocks within its catchment. This is reflected in the lowest reported signatures $\delta^{14}\text{C}$ for a small mountainous river (43 to 71 percent modern carbon), with rock-derived carbonate constituting a ^{14}C -free DIC source. Using an inverse modelling approach integrating riverine major dissolved ion chemistry and $\delta^{14}\text{C}$, we provide quantitative constraints of mineral weathering pathways and calculate atmospheric CO_2 fluxes resulting from the erosion of the Taiwan orogeny over geological timescales. The results reveal that weathering on Taiwan releases $0.31 \pm 0.12 \text{ MtC/yr}$, which is offset by burial of terrestrial biospheric organic carbon in offshore sediments. The latter tips the balance with respect to the total CO_2 budget of Taiwan such that the overall system acts as a net sink, with $0.24 \pm 0.13 \text{ MtC/yr}$ of atmospheric CO_2 consumed over geological timescales.

Taiwan is one of the most rapidly uplifting orogens, with erosion rates in the order of 3–6 mm/yr continuously exposing fresh minerals for chemical weathering^{1,2}. Together with volcanic activity, metamorphic degassing, and the organic carbon cycle, chemical weathering of minerals exerts a key control on atmospheric chemistry over geologic timescales³. Orogenies sustain high rates of physical erosion and are classically invoked as major CO_2 sinks due to the weathering of silicates by carbonic acid^{4,5}. While carbonic acid as a weathering agent is widely considered the most important, recent work has highlighted that sulphuric acid weathering of carbonates plays an important role in catchments that contain abundant pyrite^{2,6–9} and acts as a major source of CO_2 to the atmosphere over geological timescales^{10–12}. Pyrite oxidises to sulphuric acid giving rise to river dissolved sulphate^{6,8} following the weathering pathway¹⁰:



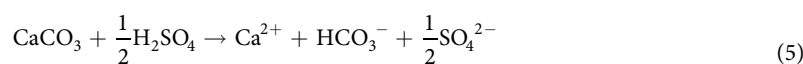
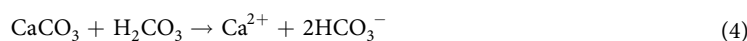
Together with carbonic acid and sulphuric acid stemming from weathering reaction (1), silicate and carbonate mineral weathering proceeds as follows



¹Geological Institute, ETH Zurich, Sonneggstrasse 5, 8092, Zurich, Switzerland. ²Department of Geosciences, National Taiwan University, No. 1, Sec. 4, Roosevelt Rd, Taipei, 10617, Taiwan. ³Department of Oceanography, National Sun Yat-sen University, 70 Lienhai Rd., Kaohsiung, 80424, Taiwan. ⁴Ion Beam Physics, ETH Zurich, Otto-Stern-Weg 5, 8093, Zurich, Switzerland. ⁵National Museum of Natural Science, No. 1, Guanqian Rd., Taichung, 40453, Taiwan. ⁶Institute for Geotechnical Engineering, ETH Zurich, Stefano-Francini-Platz 3, 8093, Zurich, Switzerland. Correspondence and requests for materials should be addressed to T.M.B. (email: thomas.blattmann@erdw.ethz.ch)

Mineral type	Weathering Pathway	HCO ₃	SO ₄	pMC	Na	Ca	Mg
					(HCO ₃ + SO ₄)	(HCO ₃ + SO ₄)	(HCO ₃ + SO ₄)
Silicate	Carbonic acid	2	0	100	0.42	0.15	0.11
	Sulphuric acid	0	1	Undef.	0.85	0.30	0.21
Carbonate	Carbonic acid	2	0	50	0.006	0.33	0.17
	Sulphuric acid	1	0.5	0	0.007	0.44	0.22

Table 1. Theoretical stoichiometries of weathering reactions and their DI¹⁴C fingerprints. Bicarbonate and sulphate concentrations normalised to one silicate or carbonate mineral unit (Ca, Mg, 2Na, 2K)SiO₃ or (Ca, Mg, 2Na, 2K)CO₃ following Eqs (2–5). The theoretical average major anion molar concentration-normalised sodium, calcium, and magnesium concentrations are given for the different mineral types and their weathering pathways.



The trails of evidence of these weathering reaction pathways (2–5) lead to unique signatures in the dissolved ion load (see Table 1). The theoretical radiocarbon isotopic composition of DIC (hereafter DI¹⁴C) arising from these pathways are characteristic for different weathering mechanisms. In reaction (2), carbon is sourced primarily from the atmosphere, which exhibits a modern signature, expressed as 100% modern carbon (pMC). Reaction (3) does not involve carbon and only adds sulphate to the dissolved river load. In reaction pathway (4), 50% of bicarbonate carbon is sourced from the atmosphere and the other half from the radiocarbon-dead lithosphere, hence characterised by a pMC = 50 “fingerprint”, while in the case of (5), bicarbonate is entirely derived from the radiocarbon-dead lithospheric source (i.e., pMC = 0). Radiocarbon has considerable advantages over stable carbon isotopic compositions of DIC by incorporating a correction for fractionation and exhibiting lower end-member uncertainty^{13,14}. Additionally, the weathering of silicates and carbonates release characteristic assemblages of major cations (calcium, magnesium, and sodium) to the river dissolved load that are further indicative of the mineral species undergoing chemical weathering⁵.

Globally, the reaction pathway of silicates and carbonates dictates the net effect of weathering on atmospheric CO₂^{3,4}, with the dissolution of carbonates by sulphuric acid acting as a CO₂ source over geological time scales¹⁰. Using a novel approach, we quantitatively disentangle the inputs of silicate and carbonate weathering via carbonic and sulphuric acid dissolution by determining DI¹⁴C and dissolved ion compositions within the Gaoping River catchment of Taiwan, leading to new quantitative estimates on the effect of the Taiwan orogeny on atmospheric chemistry.

Study Area and Methods

The Gaoping River covers a length of 170 km and drains 3257 km² in southwest Taiwan and is the island’s second largest river as measured by sediment discharge^{6,15}. Nearly half of its catchment is situated above 1000 m elevation, reaching a maximum of 3997 masl¹⁵. Within the catchment, (meta) sedimentary rocks ranging from shales to conglomerates of ages spanning from the Mesozoic to Pleistocene are exposed (see appendix for details and references). Due to the monsoonal climate, >90% of river discharge takes place in the flood season (focused in June to October)¹⁵.

Surface water samples were collected from the Gaoping River catchment during the dry season in February 2017 and 2018 as well as during the wet season in June and October 2017 (Fig. 1). Filtered water samples were enclosed in 12 ml glass exetainer vials without head-space and pre-poisoned with 12 µl of dried HgCl₂ saturated solution. One and six millilitre aliquots were purged with He, acidified with 150 µl 85% H₃PO₄, and measured for their DI¹³C and DI¹⁴C isotope compositions, respectively, using online CO₂ sparging-mass spectrometry setups described elsewhere^{16,17}. Radiocarbon values are reported in units pMC¹⁸. Concentrations of major cations and anions were measured by ion chromatography with details reported in the appendix. Bicarbonate concentrations were calculated by charge balance, following previous Taiwanese river studies^{2,8,12,19}. Inputs from rainwater were removed by assuming all chloride is sourced from the atmosphere and by subtracting ions using ratios typical for rainwater (Ca/Na = 0.023; Mg/Na = 0.11; Cl/Na = 1.15; S/Na = 0.06; HCO₃/Na = 0.004)^{5,7}.

Using a constrained linear least-squares approach with the Matlab solver lsqin, contributions from weathering reactions (2–5) are assessed from the mineral unit-normalised stoichiometries (see definition below), DI¹⁴C fingerprints, and ionic ratios characteristic for different weathering reactions listed in Table 1. Here we use α to denote the relative contributions stemming from the carbonic acid weathering of silicates ($\alpha_{\text{Silicate,H}_2\text{CO}_3}$) and carbonates ($\alpha_{\text{Carbonate,H}_2\text{CO}_3}$) and sulphuric acid weathering of silicates ($\alpha_{\text{Silicate,H}_2\text{SO}_4}$) and carbonates ($\alpha_{\text{Carbonate,H}_2\text{SO}_4}$). The model output is bound by three equality constraints: (1) the sum of the weathering contributions α_i for the mineral-normalised ion concentrations for the four reactions equals 100%, (2) measured and modelled mineral unit-normalised SO₄ must be equal, and (3) the measured and modelled DI¹⁴C must be equal. Additional constraints are included to find the best least-squares fit between modelled and measured dissolved major ion

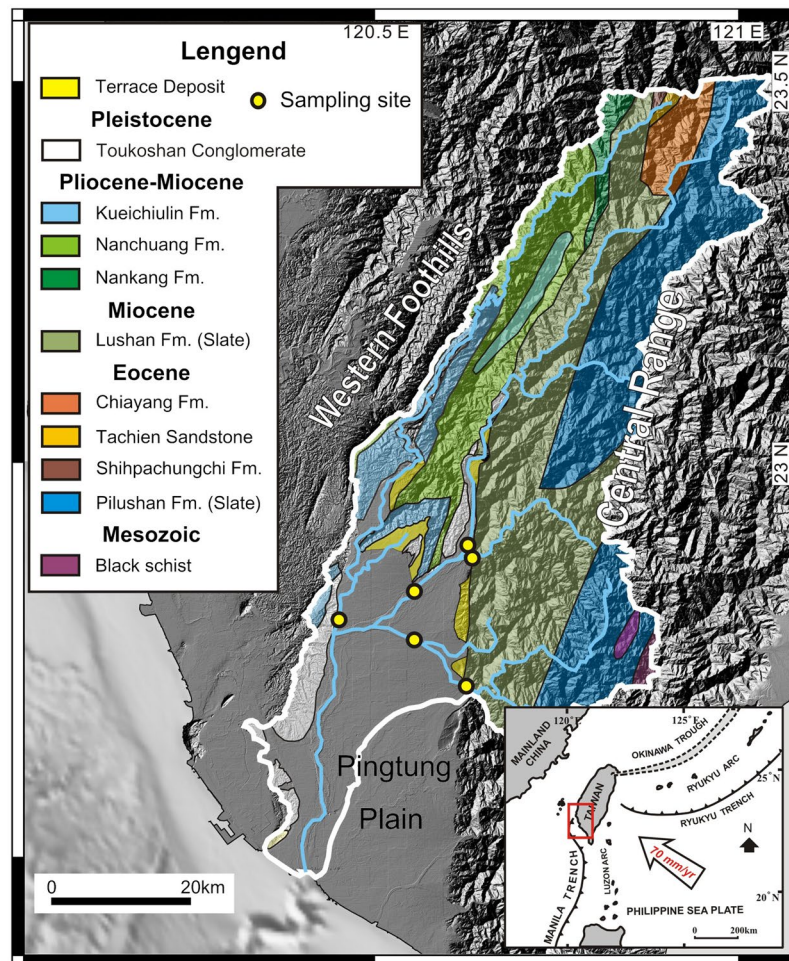


Figure 1. Gaoping River catchment. Geological and hydrological overview with sampling locations. Redrawn after geologic map of Taiwan⁴⁴, which is openly accessible (<https://data.gov.tw/dataset/11004>). Topographic features were added from open access digital elevation data (<https://data.gov.tw/dataset/35430>) and shaded with QGIS (QGIS Development Team (2018). QGIS Geographic Information System. Open Source Geospatial Foundation Project. www.qgis.org). The Gaoping River catchment was outlined from open access data from the Taiwanese government (<https://www.wra07.gov.tw/12594/12595/12602/12605/70918/>) and the final figure was generated with CorelDRAW (www.coreldraw.com).

composition based on ratios between calcium, magnesium, and sodium and the sum of sulphate and bicarbonate, which are indicative of different weathering pathways from silicates and carbonates (see Table 1 and appendix for equations). Here, we define a “mineral unit” as $(Ca, Mg, 2Na, 2K)SiO_3$ for silicates and $(Ca, Mg, 2Na, 2K)CO_3$ for carbonates. Within each silicate and carbonate mineral unit, calcium is interchangeable with charge balance equivalent amounts of magnesium, sodium, and potassium. For silicates, the relative molar abundances of these cations are typically 0.35 ± 0.25 for Ca/Na and 0.25 ± 0.2 for Mg/Na. For carbonates, Ca/Na and Mg/Na are 60 ± 30 and 30 ± 15 , respectively^{5,7}, with the uncertainties taken to represent 2- σ uncertainty in the model. Potassium is also present in carbonate mineral lattices in minor quantities ($Ca/K \approx 250\text{--}350$)²⁰, besides its presence in micas and potassic feldspars. Based on these ratios and the ideal mineral unit definition introduced here, the average formula for carbonates and for silicates is $Ca_{0.66}Mg_{0.33}Na_{0.011}K_{0.0055}CO_3$ and $Ca_{0.30}Mg_{0.21}Na_{0.85}K_{0.14}SiO_3$, respectively. Model output uncertainty was quantified by applying a Monte Carlo approach (10,000 iterations) propagating analytical uncertainties from measured ionic ratios (5% relative 1- σ uncertainty assigned), measured $\delta^{14}C$ uncertainty ($\approx 1\%$ 1- σ uncertainty based on analytical uncertainty), uncertainty in the cation composition of the weathered minerals, and uncertainty in the radiocarbon signature of the carbonic acid weathering agent. In the case of the latter, an end member signature of 100 ± 5 (1- σ uncertainty) pMC was assigned, with the uncertainty stemming from possible contributions of respired soil organic carbon^{21,22} or degraded kerogen, which attenuate the atmospheric carbon signature with the addition of bomb and aged carbon isotopic signatures. Used equations are reported in the appendix.

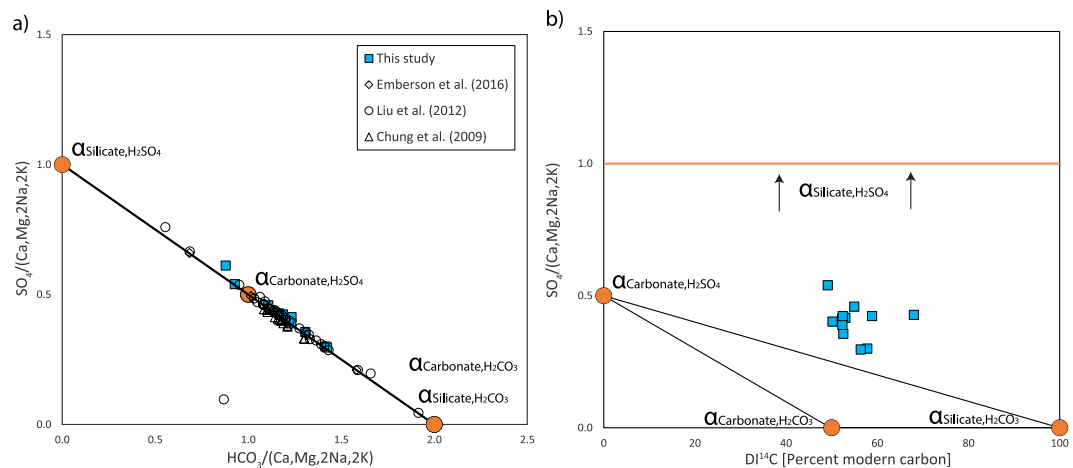


Figure 2. Mineral weathering end-member mixing. **(a)** Mineral unit-normalised sulphate versus bicarbonate abundance. The Gaoping River data collected over multiple years in relation to the quaternary end-member mixing line. Literature data points where ionic compositions reflect incursion of seawater plot away from the quaternary mixing line. One data point from this study (datapoint with highest mineral unit normalised sulphate) deviated from the mixing line due to high ammonium amounts that are attributed to anthropogenic inputs and therefore wasn't considered further in this study. Removing these anomalies, the data from this study correlates with $R^2 = 0.99$, and for all studies with $R^2 = 0.99$. **(b)** Mineral unit-normalised sulphate versus pMC of DIC. The three mineral weathering reactions producing bicarbonate span a ternary mixing triangle. All of the data lie outside of this mixing ternary due to the addition of sulphate from sulphuric acid weathering of silicates. The latter process, which leaves $DI^{14}C$ on the x-axis unaffected, adds sulphate until a theoretical maximum of one mole per weathered mineral unit, representing 100% silicate weathering by sulphuric acid.

Results and Discussion

Over the sampled time interval, pH averaged 7.9 ± 0.2 ($n = 13$) and bicarbonate represented the major anion (2.3 ± 0.6 mmol/l) followed by sulphate (0.9 ± 0.4 mmol/l) and chloride (0.2 ± 0.3 mmol/l) (supplemental Table 1). For the cations, calcium was the most abundant (1.4 ± 0.4 mmol/l $n = 13$) followed by magnesium and sodium (both 0.5 ± 0.2 mmol/l), and potassium (0.2 ± 0.2 mmol/l). Carbon isotopic compositions were centred at $-5.3 \pm 1.3\text{‰}$ for $DI^{13}C$ ($n = 13$), while $DI^{14}C$ values ranged from 43 to 68 pMC (average 54 ± 8 pMC $n = 20$) (supplemental Table 1). One sample contained 0.02 mmol/l of ammonium that was presumably sourced from anthropogenic inputs and was also characterized by the highest nitrate concentrations suggesting that nitrification induced mineral weathering was ongoing^{23,24}. As this additional weathering pathway could not be deconvolved using the approaches devised here, this sample (2018FebAR) was not considered further in this study.

Taiwanese bedrock primarily consists of (metamorphosed) sandstones, siltstones, and claystones, up to a metamorphic grade of amphibolite facies with no reports of evaporitic deposits occurring on the island²⁵ (see also Supplemental Table 2). In agreement with these geological observations, sulphur isotopes in sulphate^{6,24,26} demonstrate that pyrite oxidation is the predominant source of dissolved sulphate in Taiwanese rivers^{6,24,26}. Following the theoretical outline provided in the introduction, rainwater-corrected river data from the Gaoping River are plotted in Fig. 2a showing the mixing of the four end members, which adhere to theoretical expectations in the case of quaternary mixing of solute derived from silicate and carbonate weathering via sulphuric and carbonic acid in the absence of evaporite contributions (Fig. 2a). The relatively high concentrations of chloride ions are similar to those of New Zealand rivers within catchments that receive high amounts of precipitation, which is also attributed to cyclic salt input²⁷. Based on the measured $DI^{13}C$ values, soil organic matter and kerogen degradation are considered to contribute subordinately to the DIC pool. Similarly low contributions are also inferred for other Taiwanese rivers where most $DI^{13}C$ values suggest a predominantly carbonate source for riverine DIC¹², supporting the assumption in our model that DIC is exclusively carbonate mineral-derived. Figure 2b shows the effect of ternary mixing between reactions (2), (4), and (5). Excess sulphate is introduced into the system via reaction (3), which has no effect on the $DI^{14}C$ composition, yet causes the data points to lie outside the boundaries for ternary mixing. By applying the equations outlined in the methods and using the stoichiometric constraints summarised in Table 1 on the data reported in Table S1, the relative contributions stemming from mineral weathering pathways are calculated. These calculations deconvolve the excess sulphate contributions in order to allow quantification of the weathering contributions controlling $DI^{14}C$ under the constraint of ionic composition adhering to the quaternary mixing line. The weathering apportionment did not reveal any clear patterns as a function of sampling season or location. Averaged over the catchment and the seasons, and based on molar mineral unit-normalised weathering, $\alpha_{\text{Silicate,H}_2\text{CO}_3}$ and $\alpha_{\text{Carbonate,H}_2\text{CO}_3}$ averaged $34 \pm 5\%$ and 0.5% ($-0.5/+2\%$) respectively, while $\alpha_{\text{Silicate,H}_2\text{SO}_4}$ and $\alpha_{\text{Carbonate,H}_2\text{SO}_4}$ averaged $14 \pm 9\%$ and $53 \pm 8\%$, respectively (see also Supplemental Fig. S1–S13). Total weathered silicates ($\alpha_{\text{Silicate,H}_2\text{CO}_3} + \alpha_{\text{Silicate,H}_2\text{SO}_4}$) contribute $46 \pm 8\%$ and carbonates ($\alpha_{\text{Carbonate,H}_2\text{CO}_3} + \alpha_{\text{Carbonate,H}_2\text{SO}_4}$) contribute $54 \pm 8\%$ to the total dissolved ion load, which is broadly consistent with previous observations of major cation chemistry from the Gaoping River^{2,19,28} (see Appendix Fig. S16). Integrated over the Gaoping River catchment, the weathering effect of carbonic acid ($\alpha_{\text{Silicate,H}_2\text{CO}_3} + \alpha_{\text{Carbonate,H}_2\text{CO}_3} = 33 \pm 6\%$) and sulphuric acid

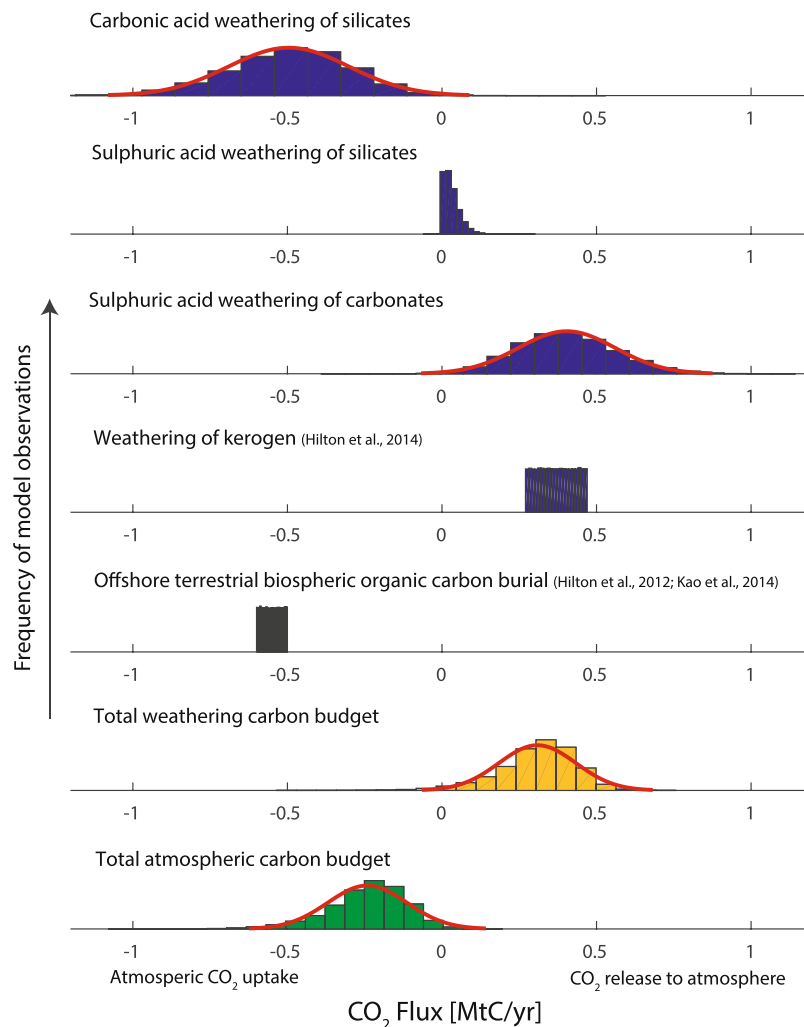


Figure 3. Fluxes of atmospheric CO₂. Net total CO₂ balance of Taiwan in MtC/yr with positive and negative values representing an atmospheric source and sink, respectively. The effects of CO₂ drawdown and release by mineral weathering (this study) and organic geochemical cycles^{29,32,33} are compared.

($\alpha_{\text{Silicate,H}_2\text{SO}_4} + \alpha_{\text{Carbonate,H}_2\text{SO}_4} = 67 \pm 6\%$) account for one-third and two-thirds of the total weathering, respectively. The results reveal that carbonates are almost exclusively weathered by sulphuric acid. This is most likely due to the limited abundance of rock carbonate (as siliclastic metasedimentary units dominate in the catchment of the Gaoping River), a high supply of sulphuric acid, and the rapid reaction kinetics of sulphuric acid with carbonates. The excess sulphuric acid continues to weather silicates. The weathering patterns observed for the Gaoping catchment operate comparably for other Taiwanese catchments including the Liwu⁸, Taimaili¹², and Chenyoulun¹² rivers. This is evidenced by their adherence to the quaternary mixing trend, encouraging the extrapolation of the results generated here to the entire Taiwan orogenic belt (see appendix).

In the case of Taiwan and major orogenic phases (e.g. Himalayan orogeny), meta-sediments are uplifted bearing the mineral ingredients to both sequester CO₂ and also release it to the atmosphere^{4,10,29}. Based on Taiwanese long-term discharge measurements (4.98×10^{13} l/yr¹), the average mineral-unit equivalent normalised dissolved ion load (2.5 ± 0.9 mmol/l $n = 63$) observed for the Gaoping River catchment (this study^{2,19,28}), and the calculated mineral weathering apportionment with propagated uncertainty, 0.50 ± 0.19 MtC/yr are removed from the atmosphere as a result of carbonic acid weathering of silicates following carbonate precipitation in the oceans. In contrast, 0.40 ± 0.16 MtC/yr are released long term as a result of sulphuric acid weathering of carbonates. While sulphuric acid weathering of silicates does not directly involve carbon, for each silicate mineral unit weathered, ≈ 0.45 mineral units of carbonate can be precipitated by combining the dissolved cations generated with bicarbonate, which then releases CO₂ to the atmosphere. Based on the ideal mineral unit formula, 0.30 moles of calcium are released upon weathering of one silicate unit and 0.66 moles of calcium are needed for one carbonate unit. Over geological timescales, sulphuric acid weathering of silicates on Taiwan may thus result in the release of 0.09 ± 0.07 MtC/yr (see second panel in Fig. 2). The net release of CO₂ to the atmosphere from chemical weathering of minerals as interpreted in this study is consistent with previous work incorporating considerations of alkalinity and DIC delivered to the ocean³⁰. CO₂ release is expected to occur on timescales longer than that of

carbonate burial (10^5 – 10^6 years), yet shorter than pyrite burial (10^7 years)³⁰ (see Fig. S14 in appendix). In addition to chemical weathering of minerals, the weathering of kerogen (CO_2 source), quantified by river dissolved rhenium, results in the release of 0.27–0.47 MtC/yr²⁹. To counterbalance this, the burial of terrestrial biospheric carbon in adjacent ocean sediments^{31,32}, quantified previously using radiocarbon as a tracer for modern sedimentary organic matter, removes 0.5–0.6 MtC/yr^{32,33}. In terms of overall carbon balance, the long-term weathering effect of silicates, carbonates, and kerogen on land, together with offshore burial of terrestrial biospheric organic carbon, results in the removal of 0.24 ± 0.13 MtC/yr from the atmosphere. However, the total weathering effect on land acts as a net source of CO_2 to the atmosphere, releasing 0.31 ± 0.12 MtC/yr (see Fig. 3). These quantities illustrate the fine balance between weathering mechanisms, and of the need to disentangle underlying processes for accurate assessment of the net effects of weathering budgets on atmospheric chemistry. The Taiwan orogeny shows that the weathering of metasedimentary catchments rich in pyrite and kerogen significantly influence the carbon budget of an orogenic entity.

The carbon budget presented here should be viewed conservatively, as two additional sources of CO_2 to the atmosphere, authigenic silicate formation³⁴ and metamorphic degassing³⁵, are not considered. Considerable uncertainty lies in the former, as this process is limited by reactive silica availability in the oceans³⁴. In the case of the latter process, the emission of CO_2 and volatile hydrocarbons (e.g. CH_4) further offset net carbon sequestration as a result of earth surface geochemical pathways and may tip the integrated surface and deep Earth geochemical cycles of an orogeny towards acting as a carbon source to the atmosphere^{35,36}. Changes through time can be expected with erosional events² as a result of major typhoons³⁷ and mineral weathering pathways modified by fertiliser usage²³. From the available data, the key variable compensating the release of CO_2 to the atmosphere due to chemical weathering is the export and preservation efficiency of terrestrial biospheric organic carbon in offshore sediments – a particularly dynamic component that is responsive to tectonic³⁸, climatic^{31,39} and anthropogenic⁴⁰ influences.

The relative importance of sulphuric acid-mediated weathering depends on the presence and weathering of pyrite in exposed lithologies. The combined contributions of the Gaoping, Mackenzie (northern Canada), and Jialing (southern China) rivers deliver around 12% of sulphide-derived sulphate to the oceans, while their catchments encompass less than 2% of the Earth's land surface⁷, highlighting the uneven distribution and localized occurrence of sulphuric acid-mediated weathering. In metasedimentary catchments such as those of the Gaoping River on Taiwan, weathering by sulphuric acid may contribute significantly to mineral dissolution. Here, it accounts for approximately two-thirds of total mineral dissolution, with carbonates almost entirely dissolved by sulphuric acid. The chemical weathering carbon budget of Taiwan supports the hypothesis that sulphuric acid mediated weathering in tandem with orogenic activity may well have affected atmospheric chemistry over geologic time¹⁰. Since the rise in atmospheric oxygen in the Precambrian, pyrite oxidation and sulphuric acid evolved therefrom has affected ocean chemistry, biologic activity, and atmospheric oxygen concentrations^{41–43}. Mineral weathering by sulphuric acid has important implications for atmospheric CO_2 inventories over geologic time^{10,30}, with CO_2 uptake and release governed by the fine balance between organic carbon burial in sediments and silicate, carbonate, and kerogen weathering controlled by the activity of oxygen, carbonic acid, and sulphuric acid. The total effect of orogenic activity on atmospheric chemistry remains a matter for discussion³⁶, yet it is clear that the presence of sulphuric acid and its involvement in carbonate and silicate mineral weathering acts as a strong buffer on atmospheric CO_2 uptake.

References

- Dadson, S. J. *et al.* Links between erosion, runoff variability and seismicity in the Taiwan orogen. *Nature* **426**, 648–651, <https://doi.org/10.1038/nature02150> (2003).
- Emberson, R., Hovius, N., Galy, A. & Odín, M. Oxidation of sulfides and rapid weathering in recent landslides. *Earth Surface Dynamics* **4**, 727–742, <https://doi.org/10.5194/esurf-4-727-2016> (2016).
- Berner, R. A. Atmospheric carbon dioxide levels over Phanerozoic time. *Science* **249**, 1382–1386, <https://doi.org/10.1126/science.249.4975.1382> (1990).
- Raymo, M. E. & Ruddiman, W. F. Tectonic forcing of late Cenozoic climate. *Nature* **359**, 117, <https://doi.org/10.1038/359117a0> (1992).
- Gaillardet, J., Dupré, B., Louvat, P. & Allègre, C. J. Global silicate weathering and CO_2 consumption rates deduced from the chemistry of large rivers. *Chemical Geology* **159**, 3–30, [https://doi.org/10.1016/S0009-2541\(99\)00031-5](https://doi.org/10.1016/S0009-2541(99)00031-5) (1999).
- Das, A., Chung, C. H. & You, C. F. Disproportionately high rates of sulfide oxidation from mountainous river basins of Taiwan orogeny: Sulfur isotope evidence. *Geophysical Research Letters* **39**, <https://doi.org/10.1029/2012GL051549> (2012).
- Burke, A. *et al.* Sulfur isotopes in rivers: Insights into global weathering budgets, pyrite oxidation, and the modern sulfur cycle. *Earth and Planetary Science Letters* **496**, 168–177, <https://doi.org/10.1016/j.epsl.2018.05.022> (2018).
- Calmels, D. *et al.* Contribution of deep groundwater to the weathering budget in a rapidly eroding mountain belt, Taiwan. *Earth and Planetary Science Letters* **303**, 48–58, <https://doi.org/10.1016/j.epsl.2010.12.032> (2011).
- Yoshimura, K. *et al.* Geochemical and stable isotope studies on natural water in the Taroko Gorge karst area, Taiwan—chemical weathering of carbonate rocks by deep source CO_2 and sulfuric acid. *Chemical Geology* **177**, 415–430, [https://doi.org/10.1016/S0009-2541\(00\)00423-X](https://doi.org/10.1016/S0009-2541(00)00423-X) (2001).
- Torres, M. A., West, A. J. & Li, G. Sulphide oxidation and carbonate dissolution as a source of CO_2 over geological timescales. *Nature* **507**, 346, <https://doi.org/10.1038/nature13030> (2014).
- Torres, M. A., Moosdorf, N., Hartmann, J., Adkins, J. F. & West, A. J. Glacial weathering, sulfide oxidation, and global carbon cycle feedbacks. *Proceedings of the National Academy of Sciences*, <https://doi.org/10.1073/pnas.1702953114> (2017).
- Emberson, R., Galy, A. & Hovius, N. Weathering of reactive mineral phases in landslides acts as a source of carbon dioxide in mountain belts. *Journal of Geophysical Research: Earth Surface*, <https://doi.org/10.1029/2018JF004672> (accepted).
- Ishikawa, N. F. *et al.* Sources of dissolved inorganic carbon in two small streams with different bedrock geology: Insights from carbon isotopes. *Radiocarbon* **57**, 439–448, https://doi.org/10.2458/azu_rc.57.18348 (2015).
- Stuiver, M. & Polach, H. A. Discussion reporting of C-14 data. *Radiocarbon* **19**, 355–363, <https://doi.org/10.1017/S0033822200003672> (1977).
- Liu, J. T., Hung, J.-J. & Huang, Y.-W. Partition of suspended and riverbed sediments related to the salt-wedge in the lower reaches of a small mountainous river. *Marine Geology* **264**, 152–164, <https://doi.org/10.1016/j.margeo.2009.05.005> (2009).

16. Breitenbach, S. F. M. & Bernasconi, S. M. Carbon and oxygen isotope analysis of small carbonate samples (20 to 100 µg) with a GasBench II preparation device. *Rapid Communications in Mass Spectrometry* **25**, 1910–1914, <https://doi.org/10.1002/rcm.5052> (2011).
17. Wacker, L. *et al.* A versatile gas interface for routine radiocarbon analysis with a gas ion source. *Nuclear Instruments and Methods in Physics Research Section B: Beam Interactions with Materials and Atoms* **294**, 315–319, <https://doi.org/10.1016/j.nimb.2012.02.009> (2013).
18. Stenström, K. E., Skog, G., Georgiadou, E., Genberg, J. & Johansson, A. A guide to radiocarbon units and calculations. **17** (2011).
19. Chung, C.-H., You, C.-F. & Chu, H.-Y. Weathering sources in the Gaoping (Kaoping) river catchments, southwestern Taiwan: Insights from major elements, Sr isotopes, and rare earth elements. *Journal of Marine Systems* **76**, 433–443, <https://doi.org/10.1016/j.jmarsys.2007.09.013> (2009).
20. Ishikawa, M. & Ichikuni, M. Uptake of sodium and potassium by calcite. *Chemical Geology* **42**, 137–146, [https://doi.org/10.1016/0009-2541\(84\)90010-X](https://doi.org/10.1016/0009-2541(84)90010-X) (1984).
21. Zheng, L.-W. *et al.* Isotopic evidence for the influence of typhoons and submarine canyons on the sourcing and transport behavior of biospheric organic carbon to the deep sea. *Earth and Planetary Science Letters* **465**, 103–111, <https://doi.org/10.1016/j.epsl.2017.02.037> (2017).
22. Hilton, R. G., Galy, A., Hovius, N., Horng, M.-J. & Chen, H. The isotopic composition of particulate organic carbon in mountain rivers of Taiwan. *Geochimica et Cosmochimica Acta* **74**, 3164–3181, <https://doi.org/10.1016/j.gca.2010.03.004> (2010).
23. Aquilina, L. *et al.* Long-Term Effects of High Nitrogen Loads on Cation and Carbon Riverine Export in Agricultural Catchments. *Environmental Science & Technology* **46**, 9447–9455, <https://doi.org/10.1021/es301715t> (2012).
24. Aquilina, L. *et al.* Autotrophic denitrification supported by biotite dissolution in crystalline aquifers (1): New insights from short-term batch experiments. *Science of The Total Environment* **619–620**, 842–853, <https://doi.org/10.1016/j.scitotenv.2017.11.079> (2018).
25. Ho, C.-S. *An introduction to the geology of Taiwan: explanatory text of the geologic map of Taiwan*. 2nd edn., 192 (Central Geological Survey, Ministry of Economic Affairs ROC, Taipei, Taiwan, 1988).
26. Pauwels, H., Ayraud-Vergnaud, V., Aquilina, L. & Molénat, J. The fate of nitrogen and sulfur in hard-rock aquifers as shown by sulfate-isotope tracing. *Applied Geochemistry* **25**, 105–115, <https://doi.org/10.1016/j.apgeochem.2009.11.001> (2010).
27. Lyons, W. B., Carey, A. E., Hicks, D. M. & Nezat, C. A. Chemical weathering in high-sediment-yielding watersheds, New Zealand. *Journal of Geophysical Research: Earth Surface* **110**, <https://doi.org/10.1029/2003JF000088> (2005).
28. Liu, Y.-C. *et al.* Boron sources and transport mechanisms in river waters collected from southwestern Taiwan: Isotopic evidence. *Journal of Asian Earth Sciences* **58**, 16–23, <https://doi.org/10.1016/j.jseaes.2012.07.008> (2012).
29. Hilton, R. G., Gaillardet, J., Calmels, D. & Birck, J.-L. Geological respiration of a mountain belt revealed by the trace element rhenium. *Earth and Planetary Science Letters* **403**, 27–36, <https://doi.org/10.1016/j.epsl.2014.06.021> (2014).
30. Torres, M. A. *et al.* The acid and alkalinity budgets of weathering in the Andes–Amazon system: Insights into the erosional control of global biogeochemical cycles. *Earth and Planetary Science Letters* **450**, 381–391, <https://doi.org/10.1016/j.epsl.2016.06.012> (2016).
31. Hilton, R. G. *et al.* Tropical-cyclone-driven erosion of the terrestrial biosphere from mountains. *Nature Geoscience* **1**, 759–762, <https://doi.org/10.1038/ngeo333> (2008).
32. Hilton, R. G. *et al.* Climatic and geomorphic controls on the erosion of terrestrial biomass from subtropical mountain forest. *Global Biogeochemical Cycles* **26** <https://doi.org/10.1029/2012GB004314> (2012).
33. Kao, S. *et al.* Preservation of terrestrial organic carbon in marine sediments offshore Taiwan: mountain building and atmospheric carbon dioxide sequestration. *Earth Surface Dynamics* **2**, 127, <https://doi.org/10.5194/esurf-2-127-2014> (2014).
34. Michalopoulos, P. & Aller, R. C. Rapid clay mineral formation in Amazon delta sediments: Reverse weathering and oceanic elemental cycles. *Science* **270**, 614, <https://doi.org/10.1126/science.270.5236.614> (1995).
35. Evans, M. J., Derry, L. A. & France-Lanord, C. Degassing of metamorphic carbon dioxide from the Nepal Himalaya. *Geochemistry, Geophysics, Geosystems* **9**, <https://doi.org/10.1029/2007GC001796> (2008).
36. Gaillardet, J. & Galy, A. Himalaya - Carbon sink or source? *Science* **320**, 1727, <https://doi.org/10.1126/science.1159279> (2008).
37. Tsai, F., Hwang, J.-H., Chen, L.-C. & Lin, T.-H. Post-disaster assessment of landslides in southern Taiwan after 2009 Typhoon Morakot using remote sensing and spatial analysis. *Natural Hazards and Earth System Sciences* **10**, 2179, <https://doi.org/10.5194/nhess-10-2179-2010> (2010).
38. Blair, N. E. & Aller, R. C. The fate of terrestrial organic carbon in the marine environment. *Annual Review of Marine Science* **4**, 401–423, <https://doi.org/10.1146/annurev-marine-120709-142717> (2012).
39. Bröder, L. *et al.* Fate of terrigenous organic matter across the Laptev Sea from the mouth of the Lena River to the deep sea of the Arctic interior. *Biogeosciences* **13**, 5003–5019, <https://doi.org/10.5194/bg-13-5003-2016> (2016).
40. Maavara, T., Lauerwald, R., Regnier, P. & Van Cappellen, P. Global perturbation of organic carbon cycling by river damming. *Nature Communications* **8**, 15347, <https://doi.org/10.1038/ncomms15347> (2017).
41. Konhauser, K. O. *et al.* Aerobic bacterial pyrite oxidation and acid rock drainage during the Great Oxidation Event. *Nature* **478**, 369, <https://doi.org/10.1038/nature10511> (2011).
42. Berner, R. A. Biogeochemical cycles of carbon and sulfur and their effect on atmospheric oxygen over Phanerozoic time. *Palaeogeography, Palaeoclimatology, Palaeoecology* **75**, 97–122, [https://doi.org/10.1016/0031-0182\(89\)90186-7](https://doi.org/10.1016/0031-0182(89)90186-7) (1989).
43. Reinhard, C. T., Lalonde, S. V. & Lyons, T. W. Oxidative sulfide dissolution on the early Earth. *Chemical Geology* **362**, 44–55, <https://doi.org/10.1016/j.chemgeo.2013.10.006> (2013).
44. Chen, C.-H. Geologic Map of Taiwan (1:500,000) *Central Geological Survey, Ministry of Economic Affairs, Taiwan R.O.C.* (2000).

Acknowledgements

We thank the participants of the ETH PhD Student Taiwan Excursion for inspiring discussions and catalysing the initiation of this study. Valier Galy is thanked for stimulating discussions. Madalina Jaggi is thanked for measurement of DI^{13}C . Fanny Leuenberger-West is thanked for measurement of dissolved ion concentrations. From National Sun Yat-sen University, we thank Yu-Shih Lin and group members for logistical support and Yuan-Pin Chang for support with sample export. The authors are indebted to three anonymous reviewers for their valuable input and to the editor Luc Aquilina for greatly improving this contribution. This work has been supported by SNF CAPS-LOCK2 Project (#200021_140850) and ETH Research Grant ETH-41 14-1.

Author Contributions

M.L., S.-L.W., T.I.E. and T.M.B. designed this study. S.-L.W., L.-H.C. and T.M.B. conducted river sampling. N.H., L.M. and T.M.B. conducted laboratory analyses and L.W. and S.M.B. provided analytical assistance. M.L., S.-L.W., S.M.B., M.P., T.I.E. and T.M.B. contributed to data analysis and interpretation. All authors provided input and comments for this manuscript.

Additional Information

Supplementary information accompanies this paper at <https://doi.org/10.1038/s41598-019-39272-5>.

Competing Interests: The authors declare no competing interests.

Publisher's note: Springer Nature remains neutral with regard to jurisdictional claims in published maps and institutional affiliations.



Open Access This article is licensed under a Creative Commons Attribution 4.0 International License, which permits use, sharing, adaptation, distribution and reproduction in any medium or format, as long as you give appropriate credit to the original author(s) and the source, provide a link to the Creative Commons license, and indicate if changes were made. The images or other third party material in this article are included in the article's Creative Commons license, unless indicated otherwise in a credit line to the material. If material is not included in the article's Creative Commons license and your intended use is not permitted by statutory regulation or exceeds the permitted use, you will need to obtain permission directly from the copyright holder. To view a copy of this license, visit <http://creativecommons.org/licenses/by/4.0/>.

© The Author(s) 2019